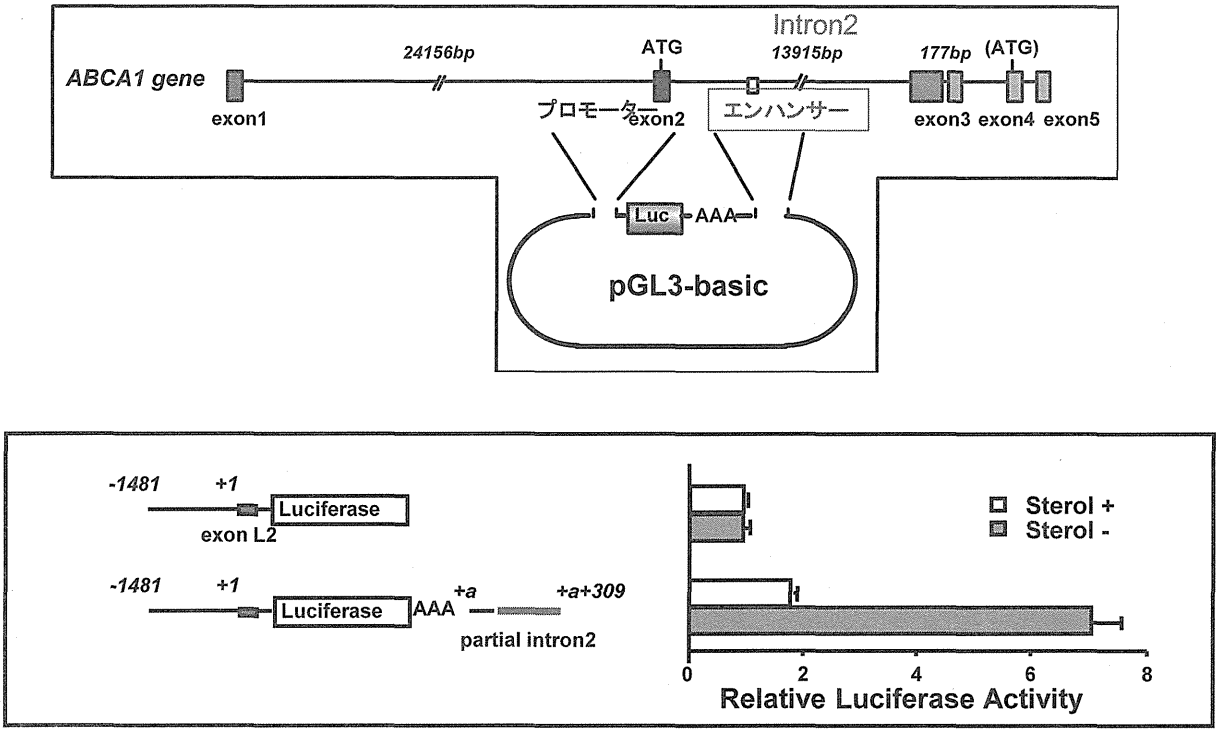

図6. ヒト肝型ABCA1 mRNAバリアントL2bプロモーター・エンハンサー領域の同定. L2b型プロモーター(exon2上流、マウス・ラット肝型プロモーターに相当)は単独ではコレステロール低下に応答しなかったが, イントロン2の部分配列約300bpをエンハンサーとして導入することにより、コレステロール低下に応答し,転写を活性化することが判明した.

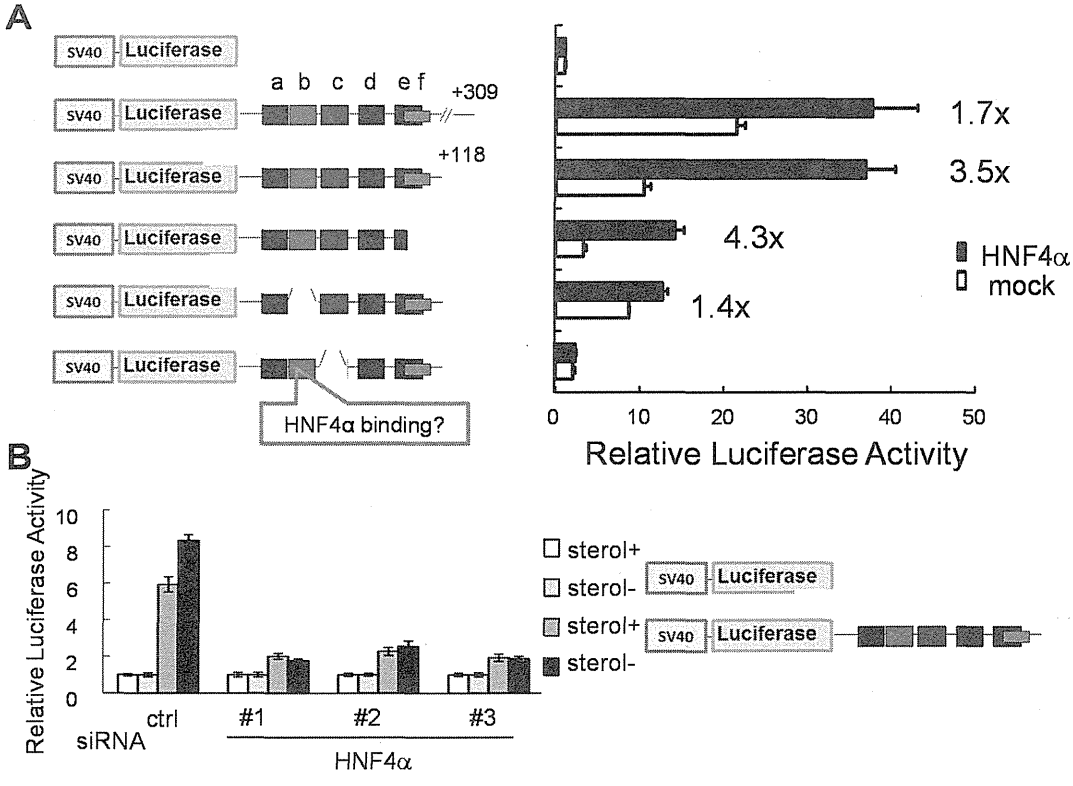

図7. ABCA1ヒト肝型 L2bエンハンサー活性はHNF4αに依存する. A. ABCA1のL2b型エンハンサーとして同定したイントロン2部分配列は, SV40プロモーターの転写活性を促進し、HNF4αを共発現するとさらに増強される。HNF4α作用にはエレメントbが必要である.
B. HNF4αをsiRNAでノックダウンするとL2bエンハンサー活性は低下する.

厚生労働科学研究委託費（創薬基盤推進研究事業）
業務委託成果研究報告書（業務項目）

担当研究課題　リポタンパク産生の解析手法の検討

担当責任者　田辺宗平　興和株式会社　東京創薬研究所　所長

研究要旨

リポタンパク機能及びリポタンパク産生トランスポーター機能の評価を行うため、コレステロール搬出能解析及び２次元電気泳動法を用いたリポタンパク性状解析の手法を検討した。方法の最適化により、血漿中 HDL のマクロファージからのコレステロール搬出能を再現性よく解析可能な測定系を確立した。また、血漿中の HDL 亜分画へのタンパク分子（apoA-I 及び apoA-II）分布を２次元電気泳動法にて解析する手法を確立した。

研究協力者
井上敬介　興和㈱東京創薬研究所　主席研究員
山崎裕之　興和㈱東京創薬研究所　主任研究員

A. 研究目的

リポタンパク機能及びリポタンパク産生トランスポーターの機能を評価するため、コレステロール搬出能解析や２次元電気泳動法を用いたリポタンパク性状解析などの手法を確立する。

B. 研究方法

(1)【コレステロール搬出能測定】マウスマクロファージ系細胞株 J774A.1 をアセチル LDL にて泡沫化させると同時に ^{3}H 標識コレステロールで細胞をラベルした。ヒト血漿をポリエチレングリコール（PEG）処理し apoB 含有リポタンパク（VLDL, LDL）を沈殿させて除去した HDL 画分を調製し、このヒト血漿由来 HDL サンプルを細胞培養系に添加したときに細胞外へ搬出されるコレステロール量を測定した。

(2)【HDL 亜分画解析】ヒト血漿サンプルをアガロースゲル電気泳動により電荷の差異で分離し（１次元目）、さらに 90 度向きを変えて 5-20%ポリアクリルアミドグラジエントゲルを用いた電気泳動で粒子径の違いにより分離した（２次元目）。２次元電気泳動で分離した HDL 亜分画中の apoA-I 及び apoA-II タンパクをウェスタンブロッティング法により検出した。

＜倫理面への配慮＞

(1) 動物実験

動物実験は本研究所の「動物実験に関する規定」に従い、興和株式会社東京創薬研究所動物実験倫理委員会の審査を受け、実施の承認を得た。

(2) ヒト由来試料の入手

ヒト由来試料については興和株式会社東京創薬研究所研究倫理審査委員会の審査を受け、研究実施及び入手の承認を得た。

C. 研究結果

C.1.　【コレステロール搬出能測定】

健常人血漿より得られたHDL画分を泡沫化したマクロファージ細胞株に添加し、4時間後に細胞内から培地中へ搬出されたコレステロール量と細胞内に残存しているコレステロール量を測定した。コレステロール搬出能の数値として、細胞内の総コレステロール量に対する細胞外へ搬出されたコレステロール量の比を算出した。さらに、各測定時に共通のコントロールサンプルをおき、このコントロールの値を100%として各測定値を補正した。図1のグラフに、2種類のヒト血漿サンプルを用いて3重測定を行い、2枚の細胞培養プレートを用いて2回別々に測定実験を行った場合のコレステロール搬出能（Cholesterol efflux）の結果を示す。グラフ中、1本のカラムに同一実験の培養プレート2枚分のデータを表示した。同一サンプルの結果を異なる培養プレート間あるいは異なる測定実験間で比較しても、ばらつきの小さい（CV値：10%以下）データを得ることができた。

C.2.　【HDL亜分画解析】

健常人血漿サンプルをアガロースゲル及びポリアクリルアミドグラジエントゲル（5-20%）にて電気泳動し、HDL亜分画中のapoA-IとapoA-IIタンパクの分布をそれぞれ検出した。2次元電気泳動法の概略を図2に示す。この方法で実施したHDL中のapoA-I及びapoA-IIの解析結果の一例を図3に示す。apoA-Iの検出結果はHDL亜分画分布そのものを示しており、実線の楕円で囲んだ部分に球状HDLであるα-1、α-2、α-3及びα-4、そして点線の円で囲んだ部分に円盤状のHDLであるPreβ-1が認められた（図3．左）。apoA-IIタンパクは、主としてα-2、α-3及びPreβ-1 HDL亜分画の位置に検出された（図3．右）。

D.考察

HDLの機能や、ABCA1、ABCG1などリポタンパク産生トランスポーターの機能を評価するため、HDLによるマクロファージからのコレステロール搬出能の測定手法を検討した。すべての測定実験に共通のコントロールサンプルをおくことにより、データのばらつきが小さく再現性のあるコレステロール搬出能評価系を確立した。今後本法を用いて、HDL機能（コレステロール搬出能）に薬剤が与える影響について解析を実施する予定である。

HDL産生及びHDLの構造・組成の解析を行うため、2次元電気泳動を用いたHDL亜分画の解析手法を検討した。HDL粒子の構成タンパクとしてもっとも重要な分子であるapoA-IとapoA-IIを、各亜分画に分離して検出する実験系を確立した。今回確立した手法は血漿サンプルのみならず、培養肝細胞などから培地中に産生されたHDLの解析にも適用することが可能と考えられる。今後は本手法を応用し、HDL粒子を構成する他のタンパク分子や脂質成分の検討を行う予定である。

E.結論

HDLの機能を解析する手法としてマクロファージからのコレステロール搬出能を再現性よく測定する方法を確立した。また、HDLの構造や組成を明らかにする手段として2次元電気泳動とウェスタンブロット法を用いたHDL亜分画（apoA-I, apoA-II）の解析方法を検討し、その手法を確立した。今回確立した手法を応用し、今後HDL粒子を構成する他のタンパク分子や脂質成分の解析手法を検討する予定である。

F. 健康危機情報

該当なし

G. 研究発表等

論文発表等

該当なし

学会発表等

該当なし

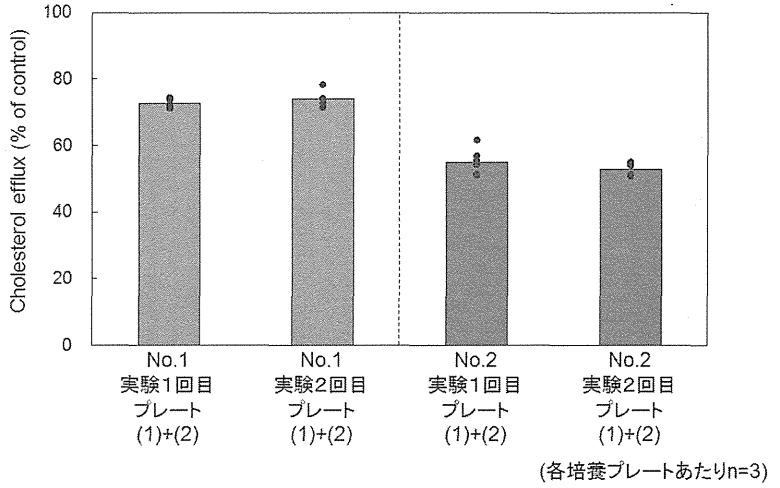

図１．HDL によるマクロファージからのコレステロール搬出能測定法の再現性

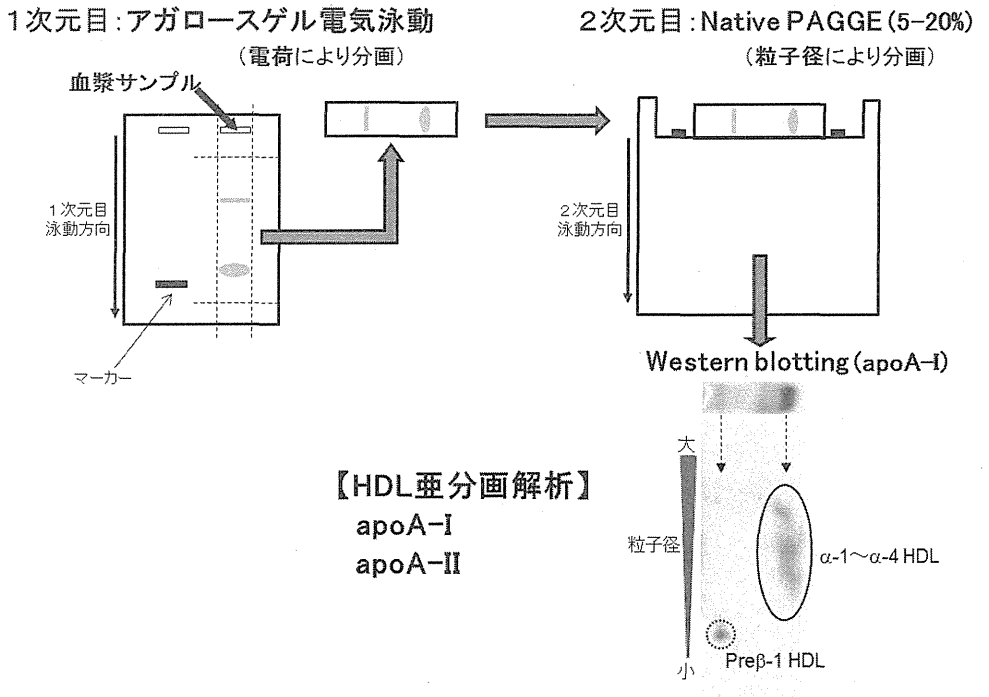

図２．２次元電気泳動法による HDL 亜分画解析の手順

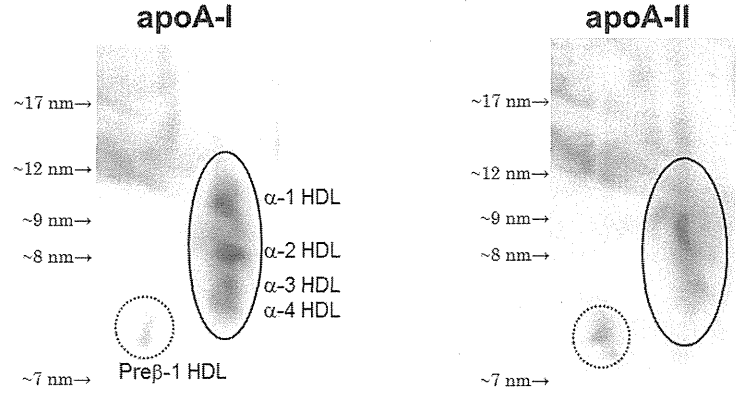

図３．HDL 亜分画解析（apoA-I 及び apoA-II を検出）

様式第１９

学　会　等　発　表　実　績

委託業務題目「医薬品・医療機器の実用化促進のための評価技術手法の戦略的開発」
機関名 国立医薬品食品衛生研究所

１．学会等における口頭・ポスター発表

発表した成果（発表題目、口頭・ポスター発表の別）	発表者氏名	発表した場所（学会等名）	発表した時期	国内・外の別
VECELL培養器を用いた肝星細胞培養の検討	石田誠一、久保崇、北條麻紀、黒田幸恵、金秀良、関野祐子	日本組織培養学会 第87回大会	2014,5	国内
胎児及び成人肝細胞のメタボローム と化学物質毒性発現の比較解析	松下琢、石井貴晃、市川雄大、金秀良、石田誠一、宮島敦子、関野祐子	日本組織培養学会 第87回大会	2014,5	国内
ヒト胎児および成人肝細胞のメタボローム解析による基礎代謝能の比較と化学物質による毒性発現の比較解析	石田誠一、金秀良、久保崇、黒田幸恵、北條麻紀、宮島敦子、松下琢、関野祐子	第41回日本毒性学会学術年会	2014,7	国内
COMPARATIVE ANALYSIS OF HUMAN FETAL AND ADULT HEPATOCYTES BY METABOLOMICS AND GENOMICS	Ishida S, Kim S, Kubo T, Kuroda Y, Ishii T, Hojyo M, Miyajima A, Matsushita T, Sekino Y.	第29回日本薬物動態学会・第19回国際薬物動態学会合同年会	2014,10	国外
ヒト肝前駆細胞HepaRGの分化過程のゲノミクス/エピジェネティクス解析	石田誠一、シュナイダー ヘレナ、久保崇、堀環、堀内新一郎、黒田幸恵	日本動物実験代替法学会 第27回大会	2014,12	国内
肝臓の代謝酵素誘導評価法の確立	石田誠一	第11回医薬品レギュラトリーサイエンスフォーラム ヒトiPS細胞を利用した安全性薬理試験法の実現に向けて	2014,12	国内
新規培養基材で培養した星細胞培養細胞LI90の機能変化の解析	石田誠一、久保崇、北条麻紀、黒田幸恵、金秀良、関野裕子	第28回肝類洞壁細胞研究会学術集会	2014,12	国内
創薬を支援する先端培養技術：PKPD予測に有用なヒト細胞の培養モデル	柿木基治	日本組織培養学会第87回大会	2014.5	国内
Hepatitis B Virus Spread in Primary-cultured Human Hepatocytes Isolated from Chimeric Mice with Humanized Liver	Ishida Y, Yamasaki C, Yanagi A, Yoshizane Y, Watashi K, Abe H, Wakita T, Chayama K, Tateno C.	2014 TASL-Japan Hepatitis B Workshop	2014.4	国外
キメラマウスから分離した初代培養ヒト肝細胞におけるHBVの水平感染	石田雄二 山崎ちひろ 吉実康美 柳愛美 山尾美香留 阿部弘美 茶山一彰 立野知世	第50回 日本肝臓学会	2014.5	国内

In vitro evaluation of fresh human hepatocytes isolated from chimeric mice with humanized livers (PXB-mice®)	Ishida Y, Yamasaki C, Yoshizane Y, Kageyama Y, Iwasaki Y, Tateno C.	第87回 組織培養学会	2014.5	国内
ヒト肝細胞キメラマウスの改良と応用. 第21回 肝細胞研究会	立野 知世	第21回 肝細胞研究会	2014.6	国内
ヒト肝細胞キメラマウス由来新鮮ヒト肝細胞を用いたHBV genotypeの性状比較	石田雄二、山崎ちひろ、吉実康美、柳愛美 田中靖人、立野知世	第21回 肝細胞研究会	2014.6	国内
ヒトALT-1特異的ELISAを用いたヒト肝細胞キメラマウスにおけるヒト肝毒性の検出	山崎ちひろ、岩成宏子、島田卓、木村達治、岩崎由美子、加国雅和、石田雄二、立野知世	第21回 肝細胞研究会	2014.6	国内
ヒト肝細胞キメラマウス肝臓におけるヒトEpCAMの発現	柳愛美、山崎ちひろ、吉実康美、石田雄二、立野知世	第21回 肝細胞研究会	2014.6	国内
ヒト肝細胞キメラマウス由来の新鮮培養ヒト肝細胞におけるHBVの水平感染	石田雄二 山崎ちひろ 吉実康美 柳愛美 山尾美香 留 阿部弘美 茶山一彰 立野知世	第10回広島肝臓プロジェクト研究センターシンポジウム	2014.7	国内
Characterization and proliferation assessment of hCK19- and hEpCAM-positive cells in bile duct-ligated chimeric mice with humanized livers	Yanagi A, Yamasaki C, Yoshizane Y, Ishida Y, Tateno C.	2014 FASEB Summer Research Conference	2014.7	国外
cDNA-uPA/SCIDマウスを用いたヒト肝細胞キメラマウスの作製および肝炎ウイルス感染	内田 宅郎, 平賀伸彦, 今村 道雄, 柘植 雅貴, 阿部弘美, 相方 浩, 石田 雄二, 立野知世, 茶山 一彰	第18回日本肝臓学会大会	2014.10	国内
超免疫不全TK-NOGマウスを用いたヒト肝細胞キメラマウス	平賀伸彦, 今村道雄, 内田宅郎, 柘植雅貴, 阿部弘美, 相方 浩, 石田雄二, 立野知世, 茶山一彰	第18回日本肝臓学会大会	2014.10	国内
In vitro evaluation of human hepatocytes isolated from chimeric mice with humanized livers (PXB-mice®). transplanted using cells from three different donors	Yamasaki C, Yanagi A, Yoshizane Y, Kageyama Y, Iwasaki Y, Ishida Y, Tateno C.	19th North American ISSX Meeting/29th JSSX Meeting	2014.10	国外
Hepatitis B virus infection efficiency and immune response decrease with cell density in primary cultured hepatocytes	Nelson CN, Abe H, Akamatsu S, Hiraga N, Imamura M, Tsuge M, Miki D, Aikata H, Ochi H, Ishida Y, Tateno C, Chayama K.	65TH AASLD	2014.11	国外
A novel humanized cDNA-iPA/SCID mouse for the study of HBV and HCV infections	Uchida T, Hiraga N, Imamura M, Tsuge M, Abe H, Hayes CN, Aikata H, Ishida Y, Tateno C, Yoshizato K, Murakami K, Chayama K.	65TH AASLD	2014.11	国外

A novel TK-NOG based humanized mouse model for the study of HBV and HCV infection	Hiraga N, Imamura M, Uchida T, Kawaoka T, Tsuge M, Abe H, Hayes CN, Aikata H, Ishida Y, Tateno C, Yoshizato K, Chayama K.	65TH AASLD	2014.11	国外
HCV kinetics in uPA-SCID chimeric mice with humanized livers during intravenous silibinin monotherapy	DebRoy S, Hiraga N, Imamura M, Canini L, Pohl RT, Persiani S, Uprichard SL, Perelson AS, Tateno C, Chayama K, Dahari H.	65TH AASLD	2014.11	国外
HBV infection in humanized chimeric mice has multiphasic viral kinetics from inoculation to steady state and an HBV half-life of 1 hr	Ishida Y, Chung TL, Imamura M, Hiraga N, Canini L, Uprichard SL, Perelson AS, Tateno C, Dahari H, Chayama K.	65TH AASLD	2014.11	国外
ヒト肝細胞移植キメラマウスを用いたCYP2D6基質のヒト体内動態予測	土居 茜, 佐能 正剛, 山崎ちひろ, 石田雄二, 加国雅和, 立野知世, 太田茂	第53回日本薬学会中国四国支部学術大会	2014.11	国内
Development of novel chimeric mice with humanized livers and infected with HBV as hosts	Tateno C.	The 11th JSH Single Ropic Conference Hepatitis B-Recent progress in basic and clinical research	2014.11	国内
ヒト肝細胞キメラマウス由来新鮮ヒト肝細胞"PXB-cellss"の性状解析	山崎ちひろ、吉実康美、柳愛美、景山豊、岩崎由美子、石田雄二、立野知世	細胞アッセイ研究会シンポジウム	2015.1	国内
ヒト肝細胞を担持するキメラ非ヒト動物	立野知世	第8回ラットリソースリサーチ研究会	2015.1	国内
ヒト肝細胞キメラマウス（PXBマウス）における卵胞発育不全	高橋美和, 立野知世, 石田雄二、井上薫, 吉田緑	第31回日本毒性病理学会	2015.1	国内

2．学会誌・雑誌等における論文掲載

掲載した論文（発表題目）	発表者氏名	発表した場所（学会誌・雑誌等名）	発表した時期	国内・外の別
Inflammatory cytokines promote the retrodifferentiation of tumor-derived hepatocyte-like cells to progenitor cells	Dubois-Pot-Schneider H, Fekir K, Coulouarn C, Glaise D, Aninat C, Jarnouen K, Le Guével R, Kubo T, Ishida S, Morel F, Corlu A.	Hepatology	2014	国外

Efficient engraftment of human iPS cell-derived hepatocyte-like cells in uPA/SCID mice by overexpression of FNK, a Bcl-xLmutant gene	Nagamoto Y, Takayama K, Tashiro K, Tateno C, Sakurai F, Tachibana M, Kawabata K, Ikeda K, Tanaka Y, Mizuguchi H.	Cell Transplant	in press	国外
Chimeric Mice with Hepatocyte-humanized Liver as an Appropriate Model to Study Human Peroxisome Proliferator-activated Receptor-α	Tateno C, Yamamoto T, Utoh R, Yamasaki C, Ishida Y, Myoken Y, Oofusa K, Okada M, Tsutsui N, Yoshizato K.	Toxicol Pathol.	in press	国外
Validation of uPA/SCID mouse with humanized liver as a human liver model: protein quantification of transporters, cytochromes P450, and UDP-glucuronosyltransferases by LC-MS/MS	Ohtsuki S, Kawakami H, Inoue T, Nakamura K, Tateno C, Katsukura Y, Obuchi W, Uchida Y, Kamiie J, Horie T, Terasaki T.	Drug Metab Dispos	2014	国外
Novel robust in vitro hepatitis B virus infection model using fresh human hepatocytes isolated from humanized mice	Ishida Y, Yamasaki C, Yanagi A, Yoshizane Y, Fujikawa K, WatashiK, Abe H, Wakita T, Hayes CN, Chayama K, Tateno C.	Am J Path.	in press	国外
Predictability of plasma concentration-time curves in humans using single-species allometric scaling of chimeric mice with humanized liver	Sanoh S, Naritomi Y, Fujimoto M, Sato K, Kawamura A, Horiguchi A, Sugihara K, Kotake Y, Ohshita H, Tateno C, Horie T, Kitamura S, Ohta S.	Xenobiotica	in press	国外
Zone analysis by two-dimensional electrophoresis with accelerator mass spectrometry of in vivo protein bindings of idiosyncratic hepatotoxicants troglitazone and flutamide bioactivated in chimeric mice with humanized liver	Yamazaki H, Kuribayashi S, Inoue T, Honda T, Tateno C, Oofusa K, Ninomiya S, Ikeda T, Izumi T, Horie T	Toxicology Research	in press	国外

（注１）発表者氏名は、連名による発表の場合には、筆頭者を先頭にして全員を記載すること。
（注２）本様式はexcel形式にて作成し、甲が求める場合は別途電子データを納入すること。

HEPATOLOGY
Official Journal of the American Association for the Study of Liver Diseases

Inflammatory Cytokines Promote the Retrodifferentiation of Tumor-Derived Hepatocyte-Like Cells to Progenitor Cells

Hélène Dubois-Pot-Schneider,[1,2] Karim Fekir,[1,2] Cédric Coulouarn,[1,2] Denise Glaise,[1,2] Caroline Aninat,[1,2] Kathleen Jarnouen,[1] Rémy Le Guével,[3] Takashi Kubo,[4] Seiichi Ishida,[4] Fabrice Morel,[1,2] and Anne Corlu[1,2,3]

Human hepatocellular carcinoma (HCC) heterogeneity promotes recurrence and resistance to therapies. Recent studies have reported that HCC may be derived not only from adult hepatocytes and hepatoblasts but also hepatic stem/progenitors. In this context, HepaRG cells may represent a suitable cellular model to study stem/progenitor cancer cells and the retrodifferentiation of tumor-derived hepatocyte-like cells. Indeed, they differentiate into hepatocyte- and biliary-like cells. Moreover, tumor-derived HepaRG hepatocyte-like cells (HepaRG-tdHep) differentiate into both hepatocyte- and biliary-like cells through a hepatic progenitor. In this study we report the mechanisms and molecular effectors involved in the retrodifferentiation of HepaRG-tdHep into bipotent progenitors. Gene expression profiling was used to identify genomic changes during the retrodifferentiation of HepaRG-tdHep into progenitors. We demonstrated that gene expression signatures related to a poor-prognosis HCC subclass, proliferative progenitors, or embryonic stem cells were significantly enriched in HepaRG progenitors derived from HepaRG-tdHep. HepaRG-tdHep retrodifferentiation is mediated by crosstalk between transforming growth factor beta 1 (TGFβ1) and inflammatory cytokine pathways (e.g., tumor necrosis factor alpha [TNFα] and interleukin 6 [IL6]). Signatures related to TNFα, IL6, and TGFβ activation pathways are induced within the first hour of retrodifferentiation. Moreover, specific activation or inhibition of these signaling pathways allowed us to determine that TNFα and IL6 contribute to the loss of hepatic-specific marker expression and that TGFβ1 induces an epithelial-to-mesenchymal transition of HepaRG-tdHep. Interestingly, the retrodifferentiation process is blocked by the histone deacetylase inhibitor trichostatin A, opening new therapeutic opportunities. *Conclusion:* Cancer progenitor cells (or metastasis progenitors) may derive from tumor-derived hepatocyte-like cells in an inflammatory environment that is frequently associated with HCC. (HEPATOLOGY 2014;60:2077-2090)

Human hepatocellular carcinoma (HCC) is the fifth most frequent cause of cancer-related deaths worldwide.[1] It is also one of the most aggressive cancers. Conventional therapies including surgical resection, liver transplantation, or chemotherapy are not very effective for this malignancy, which

Abbreviations: ALB, albumin; ALDOB, aldolase B; ANOVA, analysis of variance; BrdU, bromodeoxyuridine; CCNB1, cyclin B1; CCND1, cyclin D1; CDH1, cadherin 1 type 1 E-cadherin; CSC, cancer stem cell; CYP3A4, cytochrome P450 3A4; DMSO, dimethylsulfoxide; EMT, epithelial-to-mesenchymal transition; FC, fold change; GSEA, gene set enrichment analysis; HCC, hepatocellular carcinoma; HCV, hepatitis C virus; HepaRG-tdHep, tumor-derived HepaRG hepatocyte-like cells; IκB, I-kappa-B; IL1β, interleukin 1 beta; IL6, interleukin 6; IPA, ingenuity pathway analysis; LPS, lipopolysaccharide; NCOA3, nuclear receptor coactivator 3; NFκB, nuclear factor of kappa light peptide gene enhancer in B-cells; PGR, progesterone receptor; SERPINE1, serpin peptidase inhibitor E1; STAT3, signal transducer and activator of transcription 3; TGFβ1, transforming growth factor beta 1; TNFα, tumor necrosis factor alpha; TSA, trichostatin A.

From the [1]Inserm, UMR991, Liver Metabolisms and Cancer, F-35033 Rennes, France; [2]Université de Rennes 1, F-35043 Rennes, France; [3]ImPACcell, SFR Biosit, Université de Rennes 1, Rennes, France; [4]National Institute of Health Sciences, Division of Pharmacology, Biological Safety Research Center, Setagaya-ku, Tokyo, Japan.

Received January 20, 2014; accepted August 1, 2014.

Additional Supporting Information may be found at onlinelibrary.wiley.com/doi/10.1002/hep.27353/suppinfo.

Supported by the Institut National de la Santé et de la Recherche Médicale, the Centre National de la Recherche Scientifique, the European Commission's Seventh Framework Program under grant 223317 (LIV-ES), the Ligue contre le cancer – Comités d'Ille-et-Vilaine, des Côtes d'Armor et de Vendée, the FEDER (Fonds Européen de Développement Régional), the Contrat de plan état-région (axe biothérapie), the INSERM/Japan Society for the Promotion of Science (JSPS) Cooperation Programme, the Institut National du Cancer and the cancéropôle "Ile de France". H.D.P.S. was funded by EEC grant LIV-ES, the Contrat de plan état-région, and the Institut National du Cancer. K.F. was funded by the Conseil Régional de Bretagne and INSERM.

has a high recurrence rate of ~70%.[2] The heterogeneous nature of HCC results in drug resistance and poor prognosis of HCC. Although mature hepatocytes have long been considered the target of oncogenic transformation in HCC, it is now proposed that HCC can derive from adult hepatocytes and hepatoblasts as well as from hepatic stem/progenitors,[3] also called cancer stem cells (CSC).[4,5] Transcriptome analysis has emphasized that human HCCs show similarities with fetal hepatocytes primarily after the 22-24th week of gestation, a period of metabolic and hematopoietic shifting.[6] In addition, gene expression profiling has demonstrated the presence of a fetal hepatoblast signature in HCC with a poor prognosis.[7] A meta-analysis of nine cohorts of HCC patients (>500 HCCs) has also demonstrated a subclass of HCC (S1) with an enrichment of the progenitor/hepatoblast signature that corresponds to poorly or moderately differentiated tumors, associated with a more invasive phenotype.[8]

The origin of the hepatic stem/progenitor cells within HCC tumors is currently debated. The existence of a hepatic stem cell compartment in the normal liver has been described.[9] Therefore, resident liver stem cells can give rise to some CSCs, and their abnormal expansion and differentiation may contribute to the cellular heterogeneity in tumors. It has also been reported that progenitor cells may originate from the dedifferentiation of mature hepatocytes within the tumor.[10] In particular, the existence of hepatocyte reprogramming into atypical biliary cells leading to intrahepatic cholangiocarcinoma has been shown.[11] Recently, Holczbauer et al.[3] demonstrated that after controlled genetic transformation, all liver cell types in the hepatic lineage (adult hepatocytes, hepatoblasts, or progenitors) can undergo *in vivo* reprogramming into CSC. However, in HCC the role of mature hepatocytes in the renewal of the hepatic stem/progenitor cell pool is debated, and the mechanisms involved remain obscure.

The dedifferentiation of mature hepatocytes is primarily associated with changes in epithelial organization triggered by a epithelial-to-mesenchymal transition (EMT).[12] EMT is related to the progression of various carcinomas, including HCC,[13] and has been associated with chemoresistance.[14] The molecular mechanisms involved in EMT are well known and are mainly triggered by transforming growth factor beta (TGFβ) signaling.[15] In HCC, circulating TGFβ1 has been proposed as a biomarker for diagnosis and prognosis.[16] Moreover, in contrast to tumors expressing early TGFβ response genes (with TGFβ suppressive properties), those that express a late TGFβ signature (with TGFβ oncogenic properties) show a more aggressive phenotype and a poor prognosis.[17]

In this study we used the HepaRG cell line to characterize the molecular mechanisms contributing to the retrodifferentiation of tumor-derived hepatocyte-like cells into progenitors in HCC. HepaRG cells are derived from a hepatic, differentiated-grade 1 Edmondson tumor associated with chronic HCV infection.[18] Previously, we have shown that HepaRG cells display hepatic progenitor features and are able to differentiate into both hepatocyte and biliary lineages. Moreover, HepaRG cells that are differentiated into the hepatocyte lineage (referred to as tumor-derived HepaRG hepatocyte-like cells, or HepaRG-tdHep) express a wide variety of liver-specific genes, including major drug-metabolizing enzymes, similar to those in primary human hepatocytes.[19] Remarkably, when seeded at low density, the HepaRG-tdHep are able to differentiate into both hepatocyte- and biliary-like cells through a hepatic bipotent progenitor that retains high self-renewal ability and expresses numerous markers of early hepatic progenitors, or oval cells.[20,21] Here we show that the activation of tumor necrosis factor alpha (TNFα), interleukin 6 (IL6), and TGFβ signaling pathways directs the retrodifferentiation of HepaRG-tdHep into bipotent progenitors. These findings are consistent with the observations that associate changes in the tumor microenvironment, particularly inflammation, with the expression of EMT and stem cell markers.[22]

Materials and Methods

Cell Culture. The HepaRG cell line was cultured as previously described.[18,20] HepaRG cells were grown in William's E medium supplemented with 10% fetal bovine serum, 100 U/mL penicillin, 100 μg/mL streptomycin, 5 μg/mL insulin, and 50 μM hydrocortisone

Address reprint requests to: Anne Corlu, Ph.D., Inserm, UMR991, Liver Metabolisms and Cancer, F-35033 Rennes, France. E-mail: anne.corlu@inserm.fr; fax: +33 (0)2 99 54 01 37.

View this article online at wileyonlinelibrary.com.
DOI 10.1002/hep.27353
Potential conflict of interest: Nothing to report.

hemisuccinate. After 2 weeks the medium was supplemented with 2% dimethyl sulfoxide (DMSO) and the cells were cultured for 2 more weeks.

HepaRG-tdHep from DMSO-treated cultures were selectively detached using gentle trypsinization as previously described.[20,23] To induce retrodifferentiation, purified HepaRG-tdHep (98% positive for CYP3A4) were seeded at low density (2×10^4 cells/cm^2) in the absence of DMSO.[20] Selectively detached HepaRG-tdHep were also seeded at high density (3×10^5 cells/cm^2) in the presence or absence of DMSO, depending on the experiment. For cytokine treatments, HepaRG-tdHep were treated with the cytokines 48 hours after high-density seeding. Independent culture experiments were performed at least in triplicate.

Microarray Analysis. Messenger RNA (mRNA) from three biological replicates of each timepoint were used to perform the microarray experiment. The purity and integrity of the RNA were evaluated on an Agilent Bioanalyser (Agilent Technologies, Palo Alto, CA). Genome-wide expression profiling was performed using the GeneChip 3′ IVT Express Kit and the Human Genome U-133A Arrays (Affymetrix, Santa Clara, CA). GeneChips were scanned using the Affymetrix GeneChip Scanner 3000 7G system. The data were analyzed with Microarray Suite software v. 5.0 (MAS 5.0). The data discussed in this publication have been deposited in the NCBI Gene Expression Omnibus and are accessible through GEO Series accession number GSE52989 (http://www.ncbi.nlm.nih.gov/geo/query/acc.cgi?acc=GSE52989). Statistical analyses were performed with GeneSpring GX software v. 11.5 (Agilent Technology). Differentially expressed genes during the retrodifferentiation process (all timepoints versus timepoint 0 hours) were identified using a one-way analysis of variance (ANOVA) test with $P < 0.001$ and an absolute fold change (FC) >4. To determine the genes significantly deregulated between two timepoints, a t test (with a Benjamini-Hochberg correction) with $P < 0.05$ and FC >2 was used.

See the Supporting Materials for chemicals, reverse-transcription quantitiative polymerase chain reaction (RT-QPCR), immunocytochemistry, immunoblotting, enzyme-linked immunosorbent assay (ELISA), DNA synthesis, hierarchical clustering and annotation, ingenuity pathway analysis, gene set enrichment analysis, connectivity map, and statistical analysis.

Results

HepaRG-tdHep Retrodifferentiation Leads to the Acquisition of a Stem/Progenitor Phenotype. CYP3A4-positive HepaRG-tdHep are able to retrodifferentiate into progenitor cells without cell death.[20] To characterize the mechanisms controlling this retrodifferentiation, we performed a transcriptomic analysis at various timepoints during the retrodifferentiation process. We identified 695 significantly deregulated genes during retrodifferentiation using one-way ANOVA. Hierarchical clustering of the differentially expressed genes showed two main branches of the dendrogram associated with relevant biological functions (Fig. 1A). The upper part of the dendrogram grouped three clusters of down-regulated genes involved in 1) response to environment, 2) drug metabolism, and 3) steroid/lipid metabolic processes. The middle part of the dendrogram highlighted genes up-regulated at late timepoints of retrodifferentiation and included genes involved in the cell cycle. We confirmed by RT-QPCR that the expression of cytochrome P450 3A4 (CYP3A4), aldolase B (ALDOB), albumin (ALB), and cyclin B1 (CCNB1) involved in drug metabolism, glucose metabolism, plasma protein synthesis, and cell cycle progression, respectively, were significantly regulated during retrodifferentiation (Supporting Fig. 1A,B,D). The decrease in CYP3A4 at the protein level was also demonstrated by western blotting (Supporting Fig. 1C). The clustering validated the dedifferentiation process of HepaRG-tdHep with the loss of hepatic-specific functions followed by entry into the cell cycle. Interestingly, the lower part of the dendrogram grouped two clusters of genes up-regulated early during the retrodifferentiation. The first group corresponded to early up-regulated genes (4 hours of retrodifferentiation) related to coagulation and wound-healing functions. Among these genes, we found cyclin D1 (CCND1) expressed during the G1/S transition (Supporting Fig. 1D), as well as several serpin peptidase inhibitors (SEPINE1, SERPINE2, SERPINH1, and SERPINB1) known to inhibit fibrinolysis and TGFβ2. The second group included genes up-regulated very early during the time-course (1 hour). Interestingly, these genes are involved in cytokine activity and cell motility, including several chemokines containing C-X-C motifs (CXCL1 and CXCL10) or C-C motifs (CCL2 and CCL20), and several interleukins (IL6, IL8, and IL18) (Fig. 1A).

Unsupervised gene set enrichment analysis (GSEA) identified significant enrichment ($P < 0.01$) of signatures related to hepatoblasts or proliferative progenitors. Indeed, an enrichment of gene signatures representative of the HCC "S1 subclass" described by Hoshida et al.,[8] or the "liver cancer proliferative subclass" described by Chiang et al.,[24] were observed in HepaRG-tdHep after retrodifferentiation. In addition,

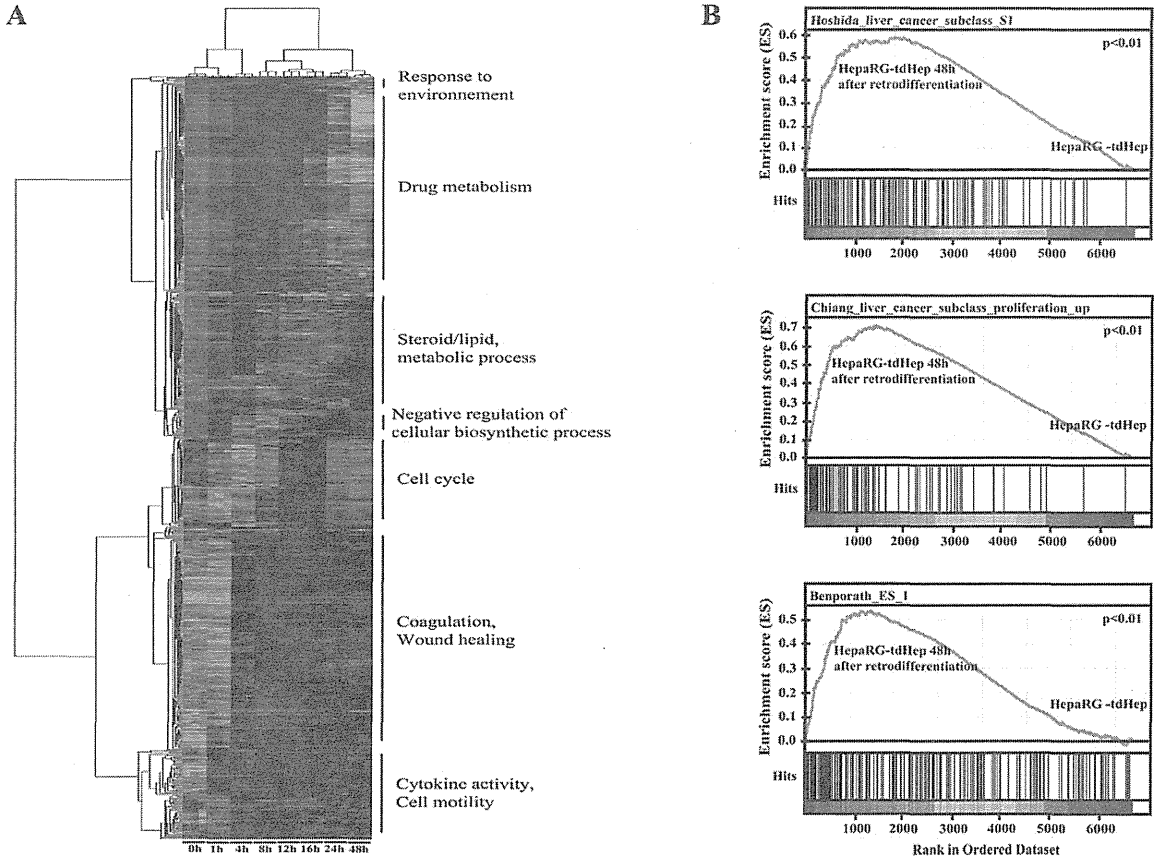

C

	0h → 1h	1h → 4h	4h → 8h	8h → 16h	16h → 24h	24h → 48h
Total	105	639	101	0	17	24
Up-regulated	102	427	30	0	15	5
Down-regulated	3	212	71	0	2	19
Top 5 functions	. Cell death . Cell growth and proliferation . Cell movement . Cell development . Gene expression	. Cell movement . Cell growth and proliferation . Cell death . Cell morphology . Cell development	. Cell movement . Cell death . Cell growth and proliferation . Cell to cell signaling and interaction . Lipid metabolism		. Cell cycle . Cellular assembly and organisation . DNA replication . Drug metabolism . Lipid metabolism	
Transcription regulators	NFκB complex	STAT3, PGR	NCOA3, IκB		FOXM1, PPARα	
Upstream regulators	TNFα, IL1β	TNFα, TGFβ1	LPS, TNFα		KDM5B, HNF4α	

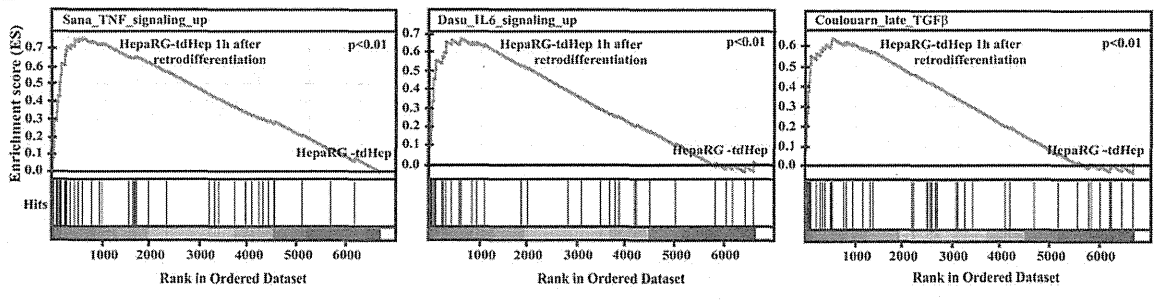

Fig. 1. Microarray data analysis. (A) Filtered microarray data were clustered with Gene Cluster 3.0 software and the clustering was visualized with Treeview. Green indicates lower expression; red higher expression. Biological functions corresponding to the main clusters were evaluated using FuncAssociate 2.0 program. (B) GSEA analysis using the gene expression profiles of HepaRG-tdHep and HepaRG-tdHep 48 hours after retrodifferentiation. GSEA revealed an enrichment of invasive, proliferative and progenitors signatures such as: the "Hoshida_liver_cancer_subclass_S1" signature (upper panel), the "Chiang_liver_cancer_subclass_proliferation_up" signature (middle panel), and the "Benporath_ES_1" signature (lower panel). (C) Number of genes significantly deregulated between two conditions ($P < 0.05$, FC >2). The top five functions, top transcription regulators, and top upstream regulators are highlighted by IPA. (D) GSEA analysis using the gene expression profiles of HepaRG-tdHep and HepaRG-tdHep 1 hour after retrodifferentiation. GSEA revealed an enrichment of the TNF signature "Sana TNF signaling up" (left panel), the IL6 signature "Dasu IL6 signaling up" (middle panel), and the TGFβ signature: "Coulouarn late TGFβ" (right panel).

signatures related to embryonic stem cells were also identified such as the Ben-Porath_ES_1 signature[25] (Fig. 1B). Accordingly, HepaRG-tdHep after retrodifferentiation gave rise to a population of stem/progenitor cells showing staining for GATA4, NANOG, cytokeratin 19 (CK19), and NODAL and expressing a range of stem/progenitors markers (Supporting Fig. 2A,B). The HepaRG-tdHep signature (48 hours versus 0 hours) was consistent with the retrodifferentiation of HepaRG-tdHep into proliferative hepatic stem/progenitors.

Commitment of HepaRG-tdHep Retrodifferentiation Involves Inflammatory Activation Pathways. The comparison of timepoint expression profiles two-by-two confirmed that gene expression changed rapidly, particularly during the early stages of retrodifferentiation (0 hours to 8 hours) (Fig. 1C). After the first hour, 102 genes were up-regulated among 105 genes whose expression was significantly modulated ($P < 0.05$, FC >2) (Supporting Table 1). During the 1-4-hour period, 639 genes were deregulated, 427 genes up- and 212 genes down-regulated (Supporting Table 2). Of note, these genes represented ~75% of all the genes modulated during the retrodifferentiation. In addition, 101 genes were significantly deregulated between 4 and 8 hours and none during the following 8-16 hours (Supporting Table 3). These genes were involved in various cellular processes, as indicated in Fig. 1C. Interestingly, ingenuity pathway analysis (IPA) revealed that the main transcriptional regulators of these genes included the nuclear factor of kappa light polypeptide gene enhancer in B-cells (NFκB) complex, the signal transducer and activator of transcription 3 (STAT3), known to mediate cellular responses to interleukins, and the progesterone receptor (PGR), as well as the nuclear receptor co-activator 3 (NCOA3) and I-kappa-B (IκB), an inhibitor of NFκB complex. IPA also showed that upstream regulators of these genes and transcription factors included the proinflammatory mediators TNFα, IL1β, and lipopolysaccharide (LPS). Consistent with these findings, unsupervised GSEA identified a significant enrichment of several signatures related to cytokine activity during the first hour of retrodifferentiation (Supporting Table 4). For instance, GSEA revealed an enrichment of the TNF signature corresponding to genes up-regulated in five primary endothelial cell types stimulated by TNF[26] and the IL6 signature found in normal fibroblasts in response to IL6.[27] A signature of genes overexpressed in primary hepatocytes at a late phase of TGFβ1 treatment and associated with a more invasive phenotype of HCC[17] was also identified (Fig. 1D). Few genes were significantly regulated at the end timepoints; between 16-24 hours or 24-48 hours, only 17 and 24 genes were differently expressed, respectively (Supporting Tables 5, 6).

The results of the transcriptomic analysis from the early timepoints prompted us to evaluate the role of the cytokines TGFβ, TNFα, and IL6 and their signaling pathways on the HepaRG-tdHep retrodifferentiation process.

Induction of TGFβ Production by HepaRG-tdHep Promotes EMT. The levels of TGFβ1 and TGFβ2 mRNA increased early during the HepaRG-tdHep retrodifferentiation (i.e., 4 hours and 1 hour, respectively) and were maintained over the time course (Fig. 2A). In accordance, the secretion of both cytokines was significantly higher 24 hours following a low-density cell seeding that allowed for retrodifferentiation, compared with a high-density cell seeding that allowed for the maintenance of hepatocyte-like functions[19] (Fig. 2B). Importantly, the presence or absence of DMSO did not affect TGFβ1 production, even though HepaRG-tdHep were derived from DMSO cultures (Supporting Fig. 3A). Associated with the TGFβ production was an increase in the expression of the primary transcription factors regulating the EMT process, SNAIL and SNAI2. This was accompanied by the induction of SERPINE1 expression, a gene associated with EMT, as well as by the repression of the epithelial marker E-cadherin (CDH1) (Fig. 2C). Cell immunostaining of HepaRG-tdHep seeded at high density and HepaRG-tdHep 24 hours after retrodifferentiation confirmed the loss of CDH1 and demonstrated the decrease of ALB along with the increase in TGFβ and SERPINE1 (Fig. 2D,E).

When A 83-01 (an inhibitor of TGFβ type I receptors) was added during the retrodifferentiation process, the expression of ALDOB and CDH1 was maintained, whereas the expression of both SERPINE1 and SNAIL was repressed (Fig. 3A). In contrast, the treatment of HepaRG-tdHep seeded at high density with human recombinant TGFβ1 induced the expression of the EMT markers SNAI2 and SERPINE1 at 4 hours (Fig. 3B). Following 2 days of treatment, cells acquired a mesenchymal morphology (Fig. 3C), and a progressive decrease in ALDOB and CDH1 expression was observed (Fig. 3B). Of note, the response to TGFβ1 treatment was not modified by the presence or absence of DMSO (Supporting Fig. 3B).

Activation of the TNFα-NFκB Pathway Triggers the Loss of Hepatic-Specific Markers. Although TNFα expression and secretion were not significantly induced during the retrodifferentiation of HepaRG-tdHep (data not shown), TNFα was identified as an

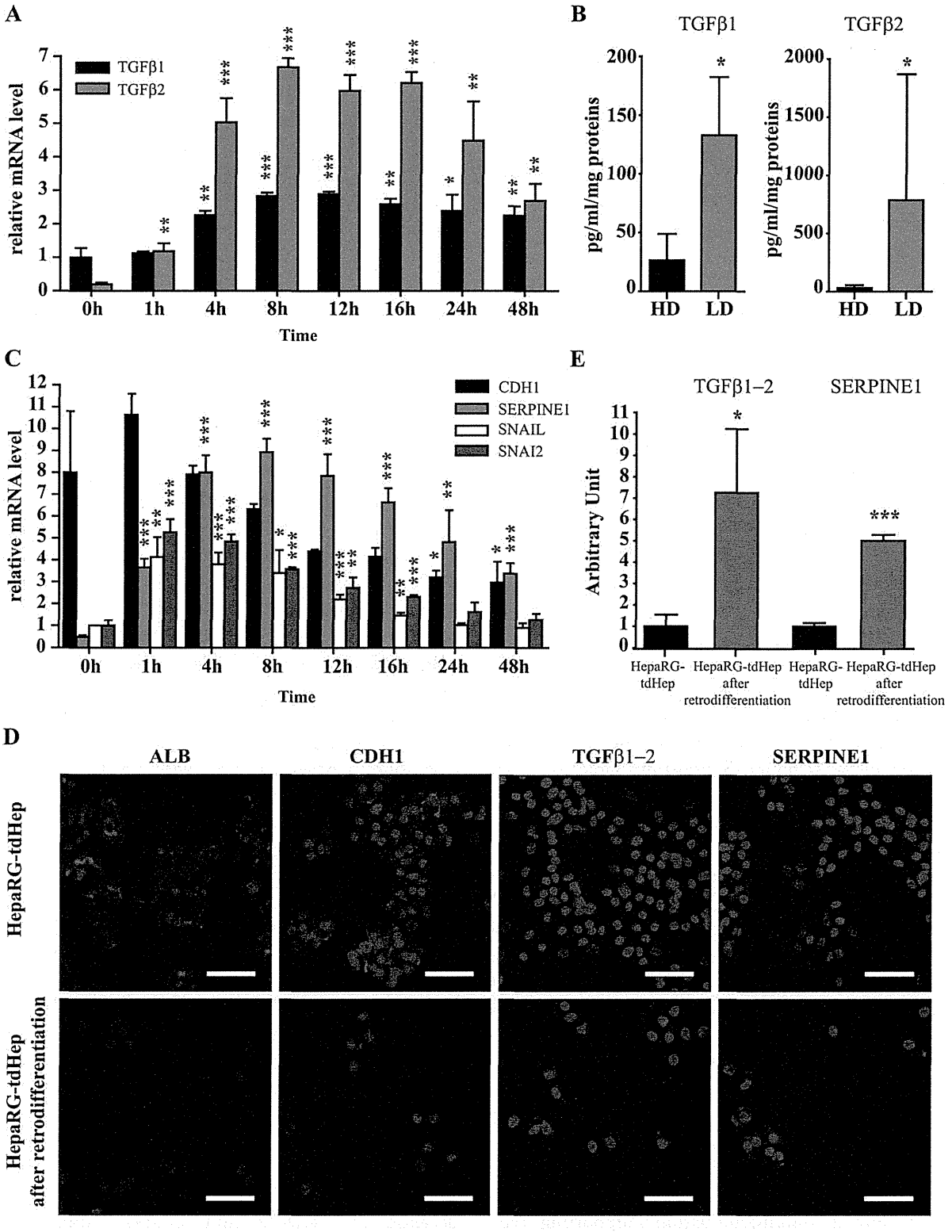

Fig. 2. Involvement of TGFβ pathway in HepaRG-tdHep retrodifferentiation. (A) mRNA levels of TGFβ1 and TGFβ2 along with the kinetic of retrodifferentiation were analyzed by RT-QPCR (n = 3). The results are expressed as relative to timepoint 0 hours, arbitrarily set to 1 for TGFβ1 and 0.2 for TGFβ2. (B) Secretion of both TGFβ1 (n = 3) and TGFβ2 (n = 4) was determined by ELISA 24 hours after high-density seeding (HD) maintaining differentiation or low-density seeding (LD) inducing retrodifferentiation. Both HD and LD seeding were performed without DMSO. (C) mRNA levels of epithelial (CDH1) and EMT (SERPINE1, SNAIL, and SNAI2) markers along the kinetic of retrodifferentiation were analyzed by RT-QPCR. The results are expressed as relative to timepoint 0 hours, arbitrarily set to 8 for CDH1, 0.5 for SERPINE1, and 1 for SNAIL and SNAI2 (n = 3). (D) Immunolocalization of ALB, CDH1, TGFβ1-2, and SERPINE1 in HepaRG-tdHep (upper panel) and HepaRG-tdHep 24 hours after retrodifferentiation (lower panel). Scale bars = 50 μm. (E) Immunolocalization quantifications for TGFβ1-2 and SERPINE1 were performed by Cell Health Profiling BioApplication from Cellomics software (n = 3). In both cases the results are expressed as relative to HepaRG-tdHep, arbitrarily set to 1. *$P < 0.05$, **$P < 0.01$, ***$P < 0.001$.

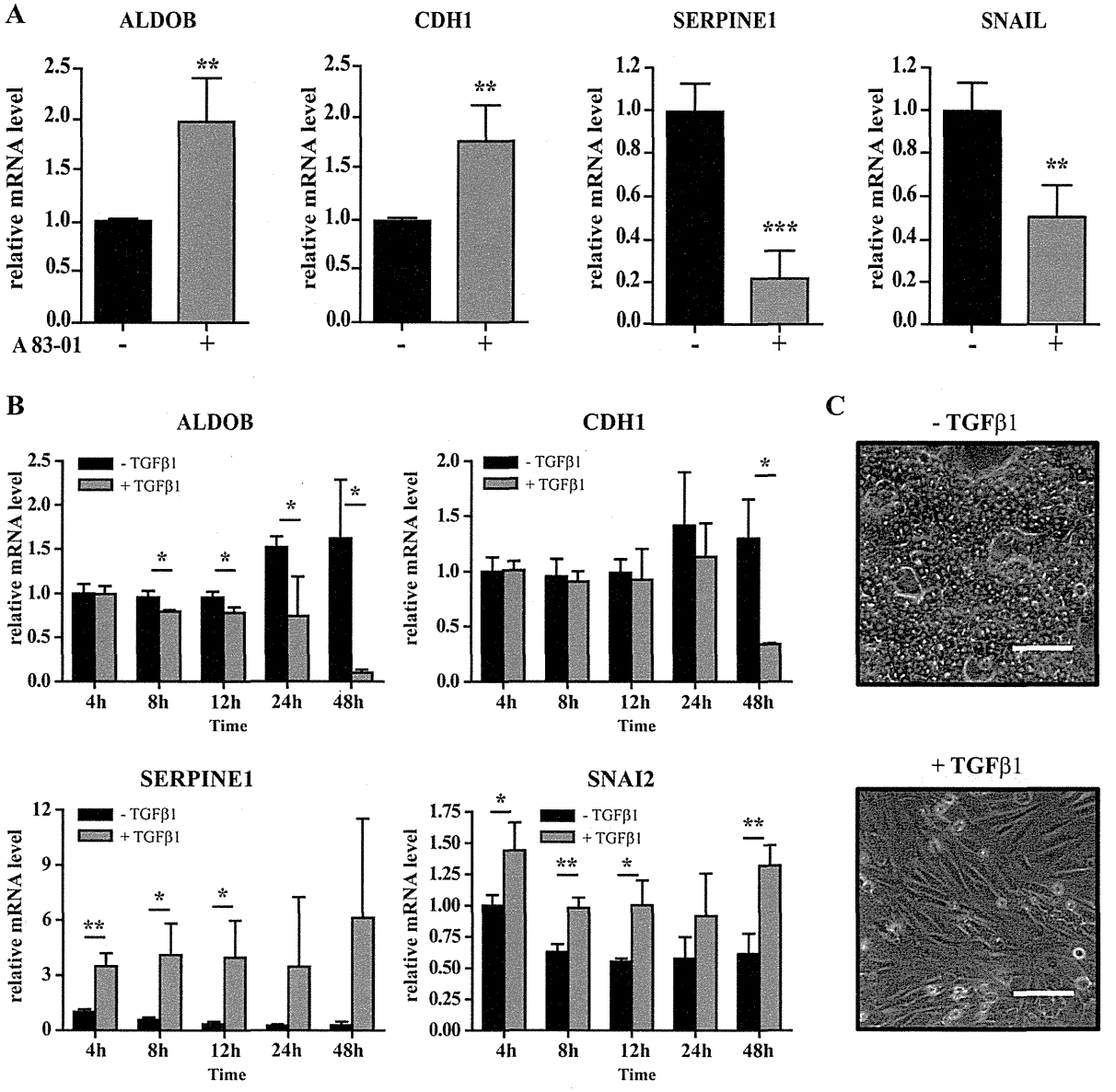

Fig. 3. TGFβ pathway contributes to HepaRG-tdHep retrodifferentiation by inducing EMT. (A) HepaRG-tdHep were seeded at a low density to induce retrodifferentiation during 24 hours in the presence or absence of 15 μM of A 83-01, an inhibitor of TGFβ type I receptor (n = 4). mRNA levels of hepatic (ALDOB), epithelial (CDH1), and EMT (SERPINE1 and SNAIL) markers were analyzed by RT-QPCR. The results are expressed as relative to those of untreated cells arbitrarily set to 1. (B) HepaRG-tdHep seeded at a high density in the presence of DMSO were treated or not with 1 ng/mL of TGFβ1 (n = 3). The mRNA levels of hepatic (ALDOB), epithelial (CDH1), and EMT (SERPINE1 and SNAI2) markers were analyzed by RT-QPCR. The results are expressed as relative to timepoint 4 hours-TGFβ1, arbitrarily set to 1. (C) Phase-contrast photographs of HepaRG-tdHep after 2 days of TGFβ1 treatment (1ng/mL). Scale bars = 100 μm. *$P < 0.05$, **$P < 0.01$, ***$P < 0.001$.

upstream regulator of numerous genes modulated during this process (Fig. 1C). IPA demonstrated that this signaling pathway was clearly activated during HepaRG-tdHep retrodifferentiation, notably by way of a gene network involving NFκB (Supporting Fig. 4). Consistent with these observations, inactivation of the NFκB pathway by SC-514, an inhibitor of the inhibitor of kappa light polypeptide gene enhancer in B-cells, kinase beta (IKK2), resulted in no changes in the expression of the hepatic and epithelial markers ALDOB and CDH1. Notably, no significant effect of SC-514 was observed on the induction of SERPINE1 and SNAIL expression (Fig. 4A). Conversely, the expression of ALDOB was significantly lower in HepaRG-tdHep seeded at high density and treated with human recombinant TNFα compared with untreated cells. Whereas CDH1 expression decreased significantly only at 12 hours, the expression of the

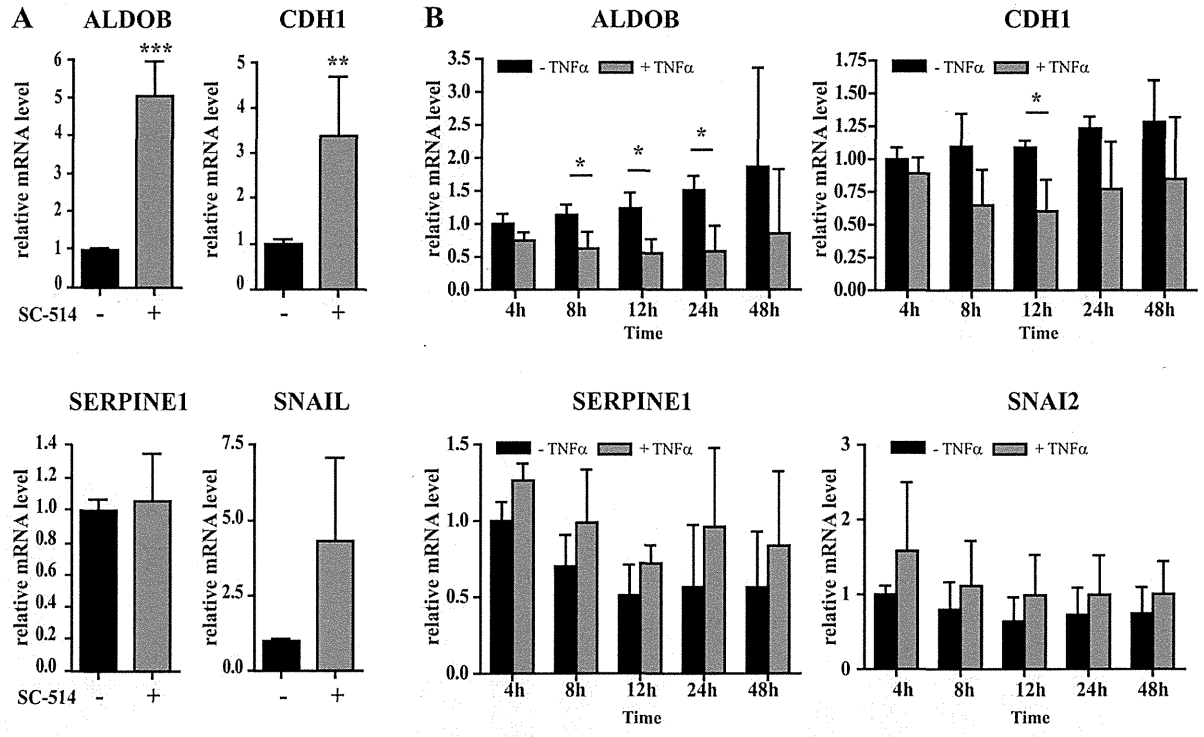

Fig. 4. TNFα pathway contributes to HepaRG-tdHep retrodifferentiation. (A) HepaRG-tdHep were seeded at a low density to induce retrodifferentiation during 24 hours in the presence or absence of 400 μM of SC-514, an inhibitor of IKK2 (n = 4). The mRNA levels of hepatic (ALDOB), epithelial (CDH1), and EMT (SERPINE1 and SNAIL) markers were analyzed by RT-QPCR. The results are expressed as relative to those of untreated cells arbitrarily set to 1. (B) HepaRG-tdHep seeded at a high density in the presence of DMSO were treated or not with TNFα (100 ng/mL) (n = 3). The mRNA levels of hepatic (ALDOB), epithelial (CDH1), and EMT (SERPINE1 and SNAI2) markers were analyzed by RT-QPCR. The results are expressed as relative to timepoint 4 hours-TNFα, arbitrarily set to 1. $*P < 0.05$, $**P < 0.01$, $***P < 0.001$.

EMT markers SERPINE1 and SNAI2 was unchanged (Fig. 4B). In addition, the presence or absence of DMSO did not affect the HepaRG-tdHep response to TNFα treatment (Supporting Fig. 3B).

IL6 Production Also Induces the Decrease of Hepatic-Specific Markers. mRNA levels of IL6 highly and rapidly increased during the retrodifferentiation (Fig. 5A). This coincided with an increase in IL6 secretion by cells committed in retrodifferentiation when compared with cells seeded at high density in the absence (Fig. 5B) or presence of DMSO (Supporting Fig. 3A). In addition, STAT3 phosphorylation 1 hour after cell seeding at low density demonstrated that the IL6 pathway was quickly activated during the retrodifferentiation (Fig. 5C). We therefore inactivated the IL6 pathway using AG490, an inhibitor of STAT3 phosphorylation, during HepaRG-tdHep retrodifferentiation. The expression of ALDOB and CDH1 was maintained in AG490-treated cells, whereas no significant changes were observed in the expression of SERPINE1 and SNAI2 (Fig. 5D). Conversely, independently of DMSO addition or removal, the treatment of HepaRG-tdHep with human recombinant IL6 induced a rapid decrease in ALDOB and CDH1 expression, whereas no significant effect on EMT markers was observed (Fig. 5E; Supporting Fig. 3B).

Crosstalk Between TGFβ, TNFα, and IL6 Pathways Induces the Retrodifferentiation of HepaRG-tdHep. We next studied the crosstalk between the three signaling pathways of TGFβ, TNFα, and IL6. In HepaRG-tdHep, TNFα treatment induced IL6 expression (Supporting Fig. 5A-C) but did not affect TGFβ1 and TGFβ2 mRNA levels (Supporting Fig. 5D). Interestingly, the treatment of HepaRG-tdHep with TGFβ1 also led to an increase in IL6 mRNA expression and secretion 8 hours after the beginning of treatment (Fig. 6A,B). In contrast, IL6 treatment had no effect on TGFβ1 and TGFβ2 expression and secretion (data not shown). We demonstrated that the treatment of HepaRG-tdHep with human recombinant TGFβ1 induced the expression of EMT and decreased the expression of hepatic markers. To determine whether this latter effect is related to IL6 induction, we simultaneously treated HepaRG-tdHep with TGFβ1 and AG490, which inhibits IL6 activity. The presence of AG490 abolished the TGFβ1-mediated reduction of

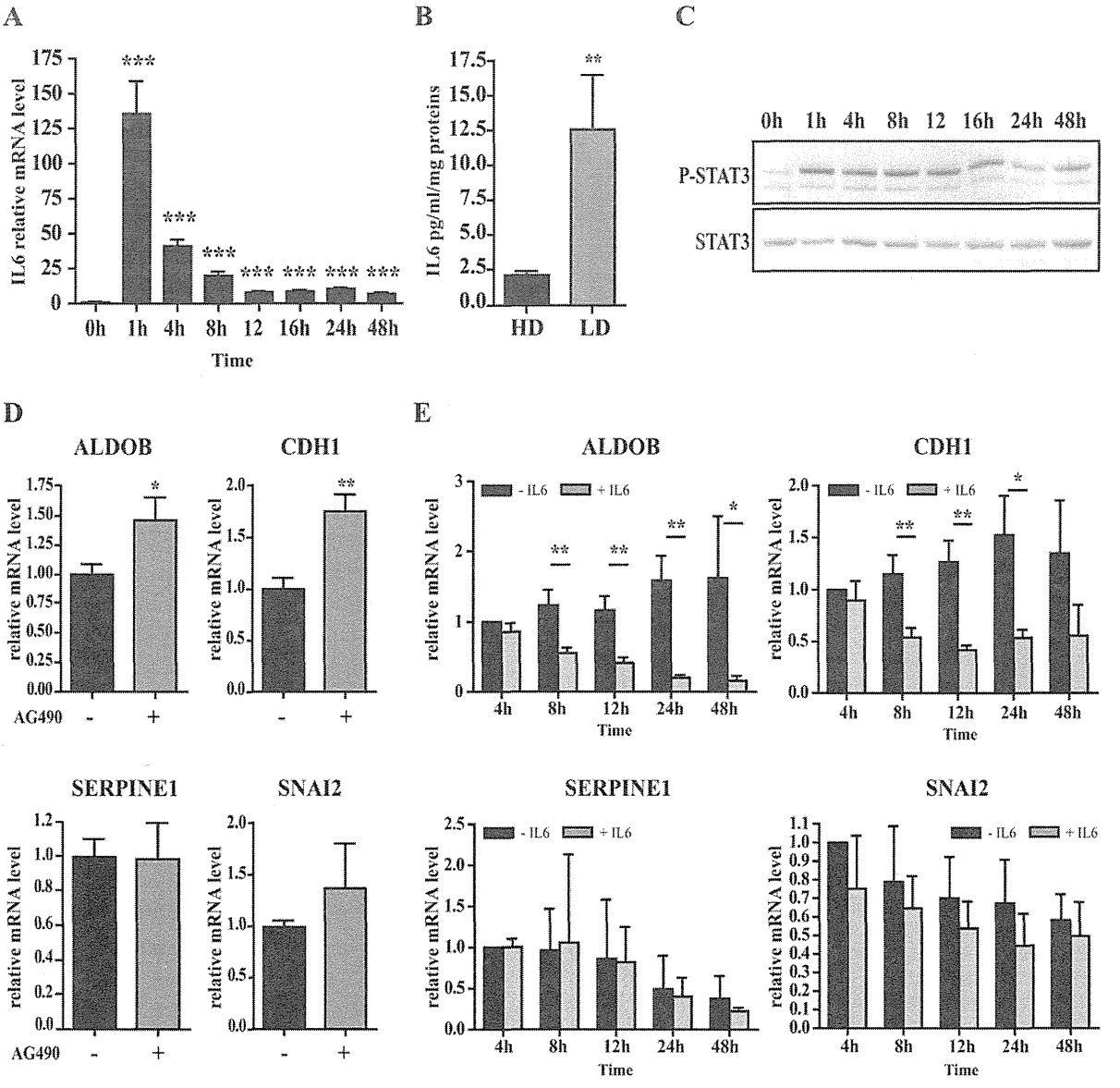

Fig. 5. IL6 pathway contributes to HepaRG-tdHep retrodifferentiation. (A) The mRNA levels of IL6 during HepaRG-tdHep retrodifferentiation were analyzed by RT-QPCR (n = 3). The results are expressed as relative to timepoint 0 hours, arbitrarily set to 1. (B) Secretion of IL6 24 hours after high-density seeding (HD) maintaining differentiation or low-density seeding (LD) inducing retrodifferentiation was determined by ELISA. Both HD and LD seeding were performed without DMSO (n = 4). (C) Western blot showing protein levels of P-STAT3 and STAT3 during HepaRG-tdHep retrodifferentiation kinetic. (D) HepaRG-tdHep were seeded at a low density to induce retrodifferentiation during 24 hours in the presence or absence of 50 μM of AG490 (n = 3). The mRNA levels of hepatic (ALDOB), epithelial (CDH1), and EMT (SERPINE1 and SNAI2) markers were analyzed by RT-QPCR. The results are expressed as relative to those of untreated cells arbitrarily set to 1. (E) HepaRG-tdHep seeded at a high density in the presence of DMSO were treated (or not) with IL6 (20 ng/mL) (n = 3). The mRNA levels of hepatic (ALDOB), epithelial (CDH1), and EMT (SERPINE1 and SNAI2) markers were analyzed by RT-QPCR. The results are expressed as relative to those at timepoint 4 hours-IL6, arbitrarily set to 1. $*P < 0.05$, $**P < 0.01$, $***P < 0.001$.

ALDOB expression, whereas it had no effect on SERPINE1 induction (Fig. 6C).

Trichostatin A Inhibits the Retrodifferentiation of HepaRG-tdHep. To identify molecules that could reverse the global gene expression profile induced during the retrodifferentiation of HepaRG-tdHep, we used a connectivity map approach as previously described.[22] Interestingly, among the top six ranked molecules, we identified five EMT inhibitors: vorinostat,[28] wortmannin,[29] LY-294002,[30] trichostatin A (TSA)[31], and resveratrol[32] (Supporting Table 7). TSA and resveratrol were then tested during the retrodifferentiation of HepaRG-tdHep. Following TSA treatment, cells maintained their hepatic morphology 24 hours after low-density cell

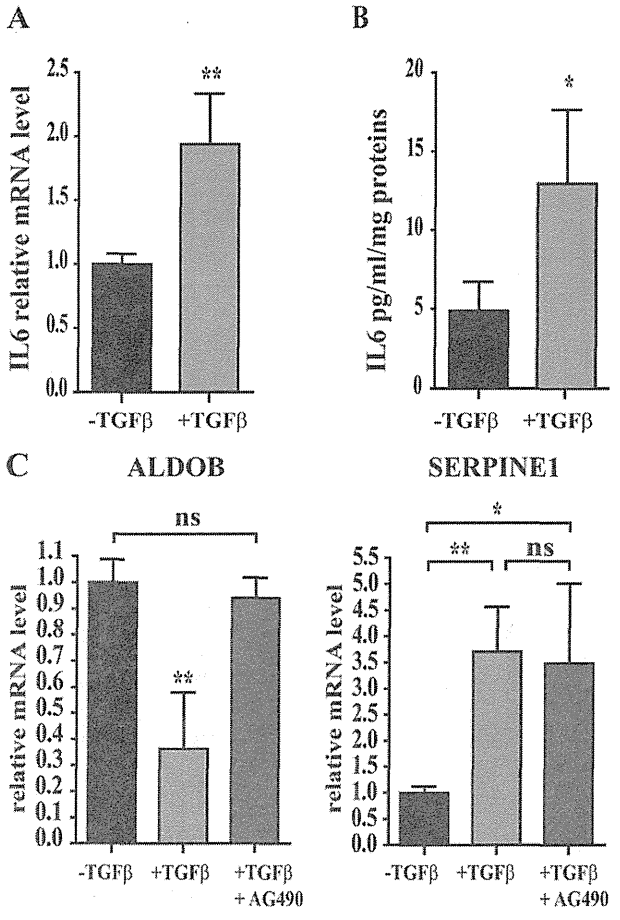

Fig. 6. Crosstalk of TGFβ and IL6 pathways. HepaRG-tdHep were seeded at a high density in the presence of DMSO. (A) The mRNA levels of IL6 after 8 hours of TGFβ1 treatment (1 ng/mL) were analyzed by RT-QPCR (n = 4). The results are expressed as relative to those of untreated cells arbitrarily set to 1. (B) Secretion of IL6 after 8 hours of TGFβ1 treatment (1 ng/mL) was determined by ELISA (n = 3). (C) HepaRG-tdHep seeded at a high density were treated for 24 hours with TGFβ1 (1 ng/mL) and 50 μM of AG490 (n = 3). The mRNA levels of hepatic (ALDOB) and EMT (SERPINE1) markers were analyzed by RT-QPCR. The results are expressed as relative to those of untreated cells arbitrarily set to 1. *$P < 0.05$, **$P < 0.01$.

seeding, compared with untreated cells that displayed extensive plasticity (Fig. 7A). In addition, the expression of ALB and CDH1 was higher in cells treated with TSA. In contrast, the expression of SERPINE1 and SNAI2 was largely repressed in the treated cells (Fig. 7B). Following resveratrol treatment, we observed the same effect, but the effectiveness of the treatment was lower than with TSA (data not shown). In addition, as demonstrated by bromodeoxyuridine (BrdU) incorporation, TSA prevented HepaRG-tdHep from entering into S-phase 48 hours after low-density seeding (Fig. 7C).

In summary, we prepared a schematic view of the molecular mechanisms that may be induced in tumor-derived hepatocyte-like cells by an inflammatory environment (Fig. 7D).

Discussion

To maintain homeostasis, inflammation is an efficient mechanism to block insults. However, persistent inflammation resulting from an infection, immune reaction, or carcinogen exposure induces multiple cell death-regeneration cycles that may favor tumor development. HCC is frequently associated with an inflammatory microenvironment,[33] and much evidence suggests that the presence of cytokines in peritumoral liver tissue or in systemic circulation leads to tumor progression and predicts late HCC recurrence and poor prognosis.[34,35] In the present study, we propose a model in which the crosstalk between the inflammatory cytokines TNFα, IL6, and TGFβ promotes HepaRG-tdHep retrodifferentiation into proliferating stem/progenitor cells. During this process, the loss of liver-specific functions, including drug and lipid metabolism, correlated with the activation of cell-cycle regulators. The induction of EMT by way of the up-regulation of specific markers SNAIL, SNAI2, and SERPINE1 and the decreased expression of the epithelial maker CDH1 correlated with early observations showing the nuclear translocation of β-catenin (CTNNB1) in HepaRG cells a few hours after low-density seeding.[20] Importantly, we demonstrated that the early phase of this process was associated with an up-regulation of genes involved in cytokine signaling and cell motility. Activation of the TNFα signaling pathway and the production of TGFβ1-2 and IL6 by HepaRG-tdHep were detected within the first hours (0-4 hours) of the process. Moreover, the treatment of HepaRG-tdHep with specific inhibitors or with recombinant cytokines promoted the involvement of these three cytokine signaling pathways in the retrodifferentiation of tumor-derived hepatocyte-like cells into progenitors. To date, few reports have demonstrated the involvement of TNFα and IL6 on hepatocyte dedifferentiation.[36] However, these cytokines have been shown to down-regulate ALB and cytochrome P450 in human primary hepatocyte cultures.[36] TNFα is an important factor for liver regeneration that also promotes tumor cell invasion. In addition, it is a key activator of IL6 through the NFκB pathway.[37,38] Consistent with these observations, TNFα treatment of HepaRG-tdHep leads to IL6 production and STAT3 phosphorylation. Interestingly, IL6 exerts many of its effects, including immune regulation, cell proliferation, and survival, by way of the activation of STAT3, a transcription factor important for HCC development.[39] Moreover, in patients with HCC a high serum level of IL6 is associated with a poor prognosis.[35] In

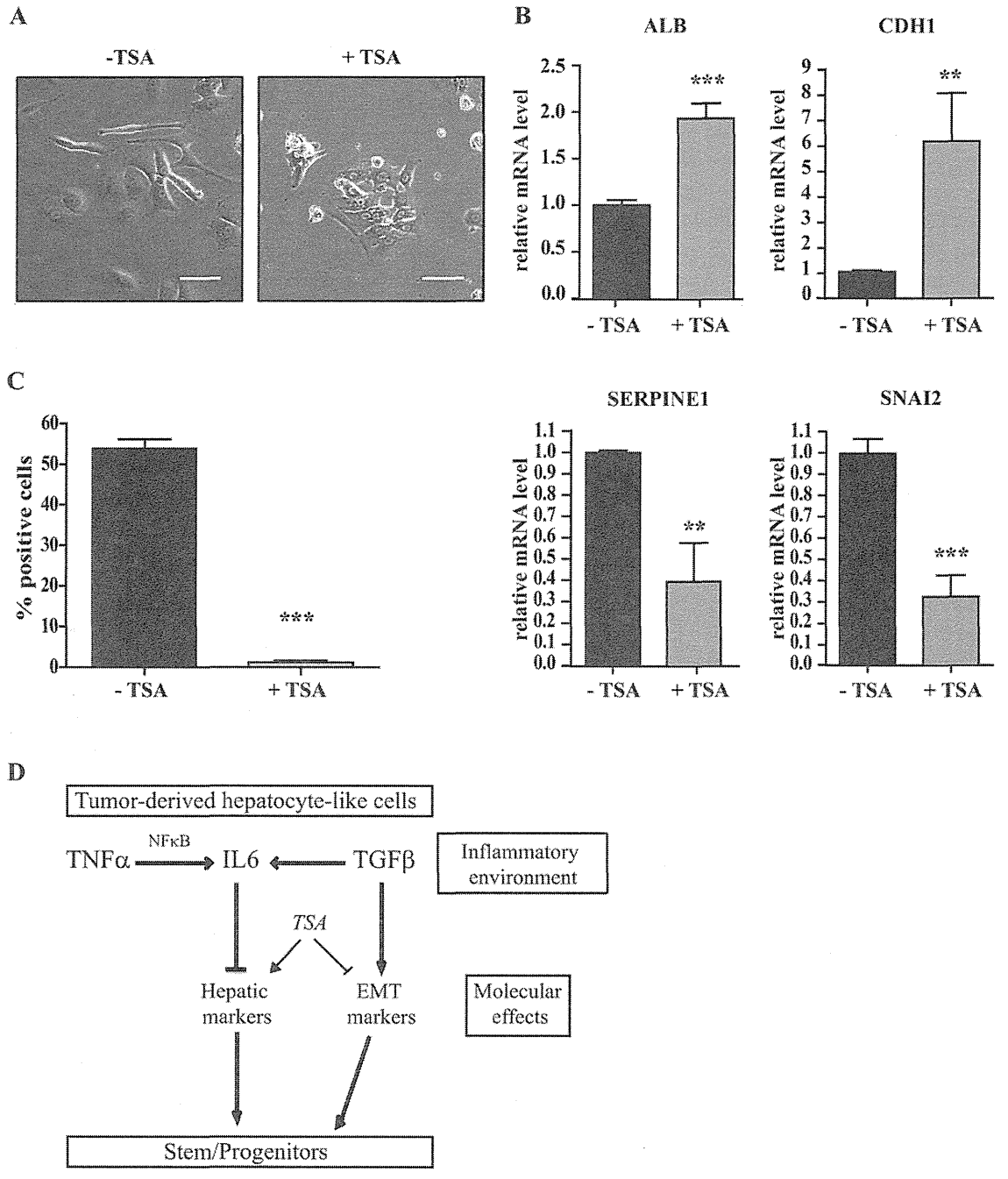

Fig. 7. TSA attenuates the retrodifferentiation of HepaRG-tdHep. (A) Phase-contrast photographs of HepaRG cells 24 hours after seeding (low density) in the presence or in the absence of 150 nM TSA. Scale bars = 100 μm. (B) The mRNA levels of hepatic (ALB), epithelial (CDH1), and EMT (SERPINE1 and SNAI2) markers 8 hours after a low-density seeding were analyzed by RT-QPCR (n = 3). The results are expressed as relative to those of untreated cells arbitrarily set to 1. (C) BrdU incorporation 48 hours after a low-density seeding and TSA treatment (n = 3). Quantification of BrdU incorporation was performed by Cell Health Profiling BioApplication from Cellomics software. (D) Schematic view of the contribution of inflammatory cytokines TNFα, IL6, and the TGFβ during HepaRG-tdHep retrodifferentiation. *$P < 0.05$, **$P < 0.01$, ***$P < 0.001$.

other cancers, TNFα and IL6 have been associated with EMT processes.[40,41] Although we observed a decrease in CDH1 expression by both cytokines, neither IL6 nor TNFα contributed to the induction of EMT markers in HepaRG-tdHep. The loss of CDH1 is typically associated with a gain of mesenchymal markers by way of a specific regulation of EMT inducers. Therefore, we cannot exclude the possibility that EMT will occur after a prolonged period of CDH1 repression. Indeed, it has been reported that